Mineralogy and Petrology (2001) 71: 225–250

Mineralogy and Petrology

Origin, spectral characteristics and practical applications of the cathodoluminescence (CL) of quartz – a review

J. Götze[1], **M. Plötze**[2], and **D. Habermann**[3]

[1] Department of Mineralogy, TU Bergakademie Freiberg, Federal Republic of Germany
[2] Department of Geotechniques, ETH Zürich, Switzerland
[3] Department of Experimental Physics, TU Bergakademie Freiberg, Federal Republic of Germany

With 7 Figures and 2 Plates

Received March 29, 2000;
accepted October 27, 2000

Summary

Investigations of natural and synthetic quartz specimens by cathodoluminescence (CL) microscopy and spectroscopy, electron paramagnetic resonance (EPR) and trace-element analysis showed that various luminescence colours and emission bands can be ascribed to different intrinsic and extrinsic defects.

The perceived visible luminescence colours in quartz depend on the relative intensities of the dominant emission bands between 380 and 700 nm. Some of the CL emissions of quartz from the UV to the yellow spectral region (175 nm, 290 nm, 340 nm, 420 nm, 450 nm, 580 nm) can be related to intrinsic lattice defects. Extrinsic defects such as the alkali (or hydrogen)-compensated [AlO_4/M^+] centre have been suggested as being responsible for the transient emission band at 380–390 nm and the short-lived blue-green CL centered around 500 nm. CL emissions between 620 and 650 nm in the red spectral region are attributed to the nonbridging oxygen hole centre (NBOHC) with several precursors.

The weak but highly variable CL colours and emission spectra of quartz can be related to genetic conditions of quartz formation. Hence, both luminescence microscopy and spectroscopy can be used widely in various applications in geosciences and techniques. One of the most important fields of application of quartz CL is the ability to reveal internal structures, growth zoning and lattice defects in quartz crystals not discernible by means of other analytical techniques. Other fields of investigations are the modal analysis of rocks, the provenance evaluation of clastic sediments, diagenetic studies, the reconstruction of alteration processes and fluid flow, the detection of

radiation damage or investigations of ultra-pure quartz and silica glass in technical applications.

Zusammenfassung

Ursachen, spektrale Charakteristika und praktische Anwendungen der Kathodolumineszenz (KL) von Quarz – eine Revision

Untersuchungen von natürlichen und synthetischen Quarzproben mittels Kathodolumineszenz (KL) Mikroskopie und -spektroskopie, Elektron Paramagnetischer Resonanz (EPR) und Spurenelementanalysen zeigen verschiedene Lumineszenzfarben und Emissionsbanden, die unterschiedlichen intrinsischen und extrinsischen Defekten zugeordnet werden können.

Die sichtbaren Lumineszenzfarben von Quarz werden durch unterschiedliche Intensitätsverhältnisse der dominierenden Emissionsbanden zwischen 380 und 700 nm verursacht. Einige der KL Emissionen vom UV bis zum gelben Spektralbereich (175 nm, 290 nm, 340 nm, 420 nm, 450 nm, 580 nm) stehen im Zusammenhang mit intrinsischen Defekten. Die kurzlebigen Lumineszenzemissionen bei 380–390 nm sowie 500 nm werden mit kompensierten [AlO_4/M^+]-Zentren in Verbindung gebracht. Die KL-Emissionen im roten Spektralbereich bei 620 bis 650 nm haben ihre Ursache im ''nonbridging oxygen hole centre'' (NBOHC) mit verschiedenen Vorläuferzentren.

Die unterschiedlichen KL-Farben und Emissionsspektren von Quarz können oft bestimmten genetischen Bildungsbedingungen zugeordnet werden und ermöglichen deshalb vielfältige Anwendungen in den Geowissenschaften und in der Technik. Eine der gravierendsten Einsatzmöglichkeiten ist die Sichtbarmachung von Internstrukturen, Wachstumszonierungen und Defekten im Quarz, die mit anderen Analysenmethoden nicht oder nur schwer nachweisbar sind. Weitere wesentliche Untersuchungsschwerpunkte sind die Modalanalyse von Gesteinen, die Eduktanalyse klastischer Sedimente, Diageneseuntersuchungen, die Rekonstruktion von Alterationsprozessen und Fluidmigrationen, der Nachweis von Strahlungsschäden oder die Untersuchung von ultrareinem Quarz und Silikaglas für technische Anwendungen.

Introduction

Quartz (low-temperature α-quartz) is one of the most abundant minerals in the Earth's crust and the most important silica mineral, occurring in large amounts in igneous, metamorphic and sedimentary rocks. Therefore, the knowledge of specific properties of quartz is important for many geological and mineralogical investigations. Moreover, the study of quartz as well as of other silica modifications has numerous practical applications: in petroleum exploration and exploitation, in hydrogeology, in the industrial minerals and rocks, in ceramics, or in archeometry (*Blankenburg* et al., 1994).

The great interest concerning luminescence studies of quartz is based on the fact, that information not available by other analytical methods can be obtained. Luminescence techniques are used to investigate and interpretate the composition and structure of minerals and their genetic characteristics and typomorphic properties (e.g., *Marfunin*, 1979; *Remond* et al., 1992; *Pagel* et al., 2000).

Cathodoluminescence (CL) can be used to reveal growth zoning in quartz crystals or to identify quartz grains from different generations of crystallization which could not be easily distinguished by optical microscopy (e.g., *Ramseyer* et al.,

1988; *Ramseyer* and *Mullis*, 1990; *Watt* et al., 1997). Important fields of application are in distinguishing igneous and hydrothermal mineralizations in igneous rocks or to discern detrital grains and authigenic overgrowths in sedimentary petrology (e.g., *Zinkernagel*, 1978; *Ramseyer* et al., 1988; *Evans* et al., 1994; *Götze*, 1996). Moreover, secondary alterations and recrystallizations can often be easily recognized using CL. Thus, it is possible to reconstruct mineral-forming processes or to trace mineral deposits.

Besides the purely descriptive way to detect and distinguish different minerals or mineral generations by their variable CL colours, the spectral analysis of CL emission is an effective method to analyze the real structure of solids (*Marfunin*, 1979). The spectral CL analysis in combination with electron paramagnetic resonance (EPR) measurements and/or spatially resolved trace-element analysis enables the investigator to detect and study extrinsic (trace elements) or intrinsic (lattice defects) point defects in minerals. The defects causing the different CL emissions in quartz often reflect the specific physico-chemical conditions of crystal growth and therefore, can be used as a signature of genetic conditions (*Ramseyer* et al., 1988; *Götze*, 1996).

Although several publications concerning the CL properties of quartz were published during the last two decades (e.g., *Trukhin* and *Plaudis*, 1979; *Entzian* and *Ahlgrimm*, 1983; *Ramseyer* et al., 1988; *Neuser* et al., 1989; *Luff* and *Townsend*, 1990; *Ramseyer* and *Mullis*, 1990; *Remond* et al., 1992; *Stevens Kalceff* and *Phillip*, 1995; *Bruhn* et al., 1996; *Demars* et al., 1996; *Gorton* et al., 1996; *Götze*, 1996; *Watt* et al., 1997), the application of new analytical techniques such as spatially and time-resolved analysis of CL emission, spatially resolved trace-element analysis (PIXE, SIMS) or the combination of CL with other advanced analytical methods (EPR, micro-Raman) brought some new insights into the real structure and luminescence behaviour of quartz. In the present work the recent state of knowledge about quartz CL is summarized including some principal ideas about the origin of the different CL properties of quartz of various origin. Furthermore, results of some practical applications of quartz CL are presented.

Materials and methods

In the present study results of extensive studies on quartz samples of certain origin are summarized. The analyzed material includes more than 500 quartz samples from all over the world of different parent rocks (igneous, metamorphic and sedimentary parent rocks) and synthetic quartz specimens. The material was analyzed by a combination of CL microscopy and high-resolution CL spectroscopy. Selected samples were further characterized by EPR measurements and trace element analysis.

CL examinations were carried out on polished thin sections using a ''hot cathode'' CL microscope. The system was operated at 14 kV and with a current density of about 10 $\mu A/mm^2$. Thin sections were coated with carbon to prevent any build-up of electrical charge during CL operation. Luminescence images were captured ''on-line'' during CL operations by means of an adapted digital video-camera (KAPPA 961-1138 CF 20 DXC with cooling stage). CL spectra were obtained using an EG&G digital triple-grating spectrograph with LN_2-cooled CCD

detector. The CCD camera was attached to the CL microscope by a silica-glass fiber-guide (cf. *Neuser* et al., 1995). CL spectra were measured in the wavelength range 320 to 800 nm using standardized conditions (wavelength calibration with a Hg lamp, intensity calibration with an external standard, spot width 30 µm). To prevent any falsification of the CL spectra due to electron bombardment, all spectra were taken on samples that were not irradiated by an electron beam before analysis. Due to absorption effects of the used glass optic and the efficiency of the detector, the spectral range < 380 nm cannot be used for detailed interpretation.

The paramagnetic centres of selected natural as well as irradiated (^{60}Co, 295 K, 2100 Gy and 10^6 Gy for Al centre saturation, respectively) quartz samples were investigated by EPR at frequencies of the X-band (about 9.5 GHz) at 20, 70 and 295 K. Before γ-irradiation the samples were heated at 400 °C for 5 h to anneal the paramagnetic centres formed by natural irradiation. Spectra were recorded by a Varian E-line spectrometer. The sample temperature was controlled with a low temperature unit based on a helium gas flow device (Oxford ESR 900A). The influence of technical parameters such as modulation amplitude, microwave power, temperature, scan time etc. on the spectra was checked for the optimal settings for recording the spectra. These settings (modulation field $H_M = 1$ G, temperature $T = 295$ K, microwave power $p = 0.2$ mW for E′ and 30 mW for oxygen-associated hole centres (O^-) and $H_M = 1\,\mathrm{G}, p = 7\,\mathrm{mW}, T = 70\,\mathrm{K}$ for $[AlO_4]^0$ centres) were kept constant throughout all the measurements to allow correct comparison between the signal intensities of different spectra. The concentration of the paramagnetic centres was determined as peak to peak or peak to base intensity at the analytical lines (*Moiseev*, 1985). The specific peak positions of the paramagnetic centres were drawn from simulated spectra and from data from the literature. The program of *Nettar* and *Villafranca* (1985) was used for the powder spectra simulations. The variation of intensity detected by repeated measurements of selected analytical lines is up to 10%. The concentration of Al centres was quantified using a reference sample with known $[AlO_4]^0$ concentration (*Moiseev*, 1985). All other centres were calculated in relative amounts.

The real structure of quartz

The real structure of minerals significantly influences their luminescence behaviour. Especially in the case of quartz, where the incorporation of activator elements is limited, the detection and characterization of lattice defects is important for the discussion of the CL properties. The type and frequency of lattice defects are influenced by the thermodynamic conditions during mineralization. On the other hand, post mineralization effects, such as metamorphism, tempering or deformation can change the structural properties of quartz. Thus, the actual structure reflects the specific conditions of formation. The lattice defects can be classified according to their structure and size as follows: point defects (most important for luminescence studies), translations, inclusions of paragenetic minerals, and gas/liquid inclusions.

In the course of quartz synthesis and by exhaustive studies of natural quartz (e.g. *Bambauer*, 1961; *Medlin*, 1962; *Marfunin*, 1979; *Weil*, 1984, 1993; *Kostov* and *Bershov*, 1987; *Agel*, 1992; *Blankenburg* et al., 1994; *Plötze*, 1995; *Götze* and *Plötze*, 1997; *Götze* et al., 1999) it has been shown that numerous displaced atoms

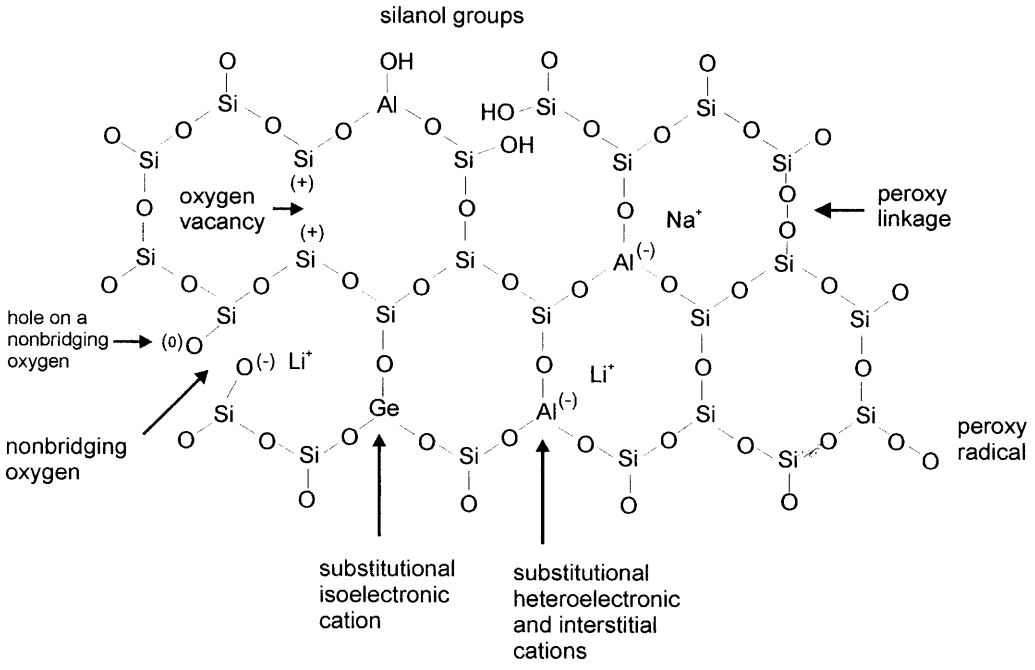

Fig. 1. Schematic quartz structure showing the most common intrinsic and extrinsic lattice defects

as well as various foreign ions are contained in quartz in regular lattice and interstitial positions. New information on the structure of such defect centres has been obtained from EPR studies either alone or in combination with other spectroscopic methods such as thermoluminescence (TL), CL, infrared spectroscopy or absorption measurements (e.g., *Weil*, 1984, 1993; *Krbetschek* et al., 1998; *Stevens Kalceff* et al., 2000 and references therein).

Generally, about 20 different types of paramagnetic defect centres were observed in quartz to date (*Weil*, 1984, 1993). They can be subdivided into two main types: (i) defects caused by foreign ions (foreign ion centres and interstitial defects) and (ii) centres associated with vacant oxygen or silicon positions (Fig. 1). In addition, several types of nonparamagnetic precursors of the paramagnetic defects were observed.

Substitution of silicon atoms in the lattice is rare because of the small ion radius of Si^{4+} (0.42 Å) and its high valence. So far Al^{3+} (0.51 Å), Ga^{3+} (0.62 Å), Fe^{3+} (0.64 Å), Ge^{4+} (0.53 Å), Ti^{4+} (0.64 Å), and P^{5+} (0.35 Å) have been detected as substitutes. Furthermore, *Nutall* and *Weil* (1980) reported a hydrogenic trapped hole-centre with four hydrogen atoms in a regular silicon lattice position. Since, in the case of some elements, compensation of the electric charge is necessary, additional cations such as H^+, Li^+, Na^+, K^+, Cu^+, Ag^+ can be incorporated in interlattice positions in conjunction with structural channels.

Aluminium is the most frequent trace element in quartz (up to a few 1000 ppm). Its diadochic incorporation into quartz can be explained by the common occurrence in the Earth's crust and by the similar ionic radii of Al^{3+} and Si^{4+}. The $[AlO_4]^0$

centre is caused by substitution of Al^{3+} for Si^{4+} with an electron hole at one of the four nearest O^{2-} ions, forming O^{1-} (*Griffiths* et al., 1954). The precursor state for this centre is the diamagnetic $[AlO_4/M^+]^0$ centre associated with an adjacent charge compensating cation M^+ (H^+, Li^+, Na^+). Quantitative determination of the Al-centre concentrations of both rock quartz and agate by EPR (*Plötze*, 1995; *Götze* and *Plötze*, 1997; *Götze* et al., 1999) showed that the concentration of bulk "trace element Al" is higher than structural "EPR Al" indicating that the trace-element input into quartz either by microinclusions or by "non-paramagnetic" Al (e.g. in structural channels) may be an important factor.

Other common trace-element centres detected in quartz by EPR are $[FeO_4/M^+]^0$, $[GeO_4/M^+]^0$ and $[TiO_4/M^+]^0$ ($M^+ = H^+$, Li^+, Na^+). Centres of the type $[TiO_4/Li^+]^0$ and $[TiO_4/H^+]^0$, detected in quartz of igneous rocks, are absent in cryptocrystalline quartz (agate) indicating different conditions of formation (*Götze* et al., 1999).

The second type of defects is attributed to the group with E′ and O^- centres, the best known of which is the E_1' centre, an oxygen vacancy centre. The oxygen tetrahedra are transformed into a planar arrangement of three oxygen ions. The centre can exist in three different stages E_1^0, E_1' and E_1'' (e.g. *Rakov* and *Moiseev*, 1977; *Jani* et al., 1983; *Halliburton* et al., 1984; *Moiseev*, 1985) corresponding to its thermal stability and to the reactivity with respect to irradiation (capture of one or two electrons possible). O^- centres represent different types of defect electrons on O^{2-} in tetrahedra with a silicon vacancy. Recent investigations have shown that the abundance of O_2^{3-} centres (silicon vacancy) and E_1' centres (oxygen vacancy) is remarkably high in cryptocrystalline quartz (agate). This high defect density in agates points to rapid growth of silica from a strongly supersaturated solution probably with a non-crystalline precursor (*Götze* et al., 1999).

The nonbridging oxygen hole center (NBOHC: ≡Si–O) is described as a hole trapped in a single oxygen atom bound to a single silicon on three oxygen atoms in the SiO_2 structure (*Griscom*, 1985). Oxygen excess centres include the peroxy radical (≡Si–O–O), an oxygen associated hole centre consisting of an O_2^- ion bonded to a single silicon on three oxygen atoms, and the peroxy linkage (≡Si–O–O–Si≡) (*Friebele* et al., 1979; *Baker* and *Robinson*, 1983). A further type of defects are OH^- centers which consist of a proton bound on a regular lattice O^{2-} ion, located between two O^{2-} ions of the SiO_4 tetrahedron (*Weil*, 1984). Because of the negative net charge, additional trivalent substitutes of the Si^{4+} positions occur as charge compensation (e.g. Al^{3+}) in such a way that an additional proton is bound on the Al^{3+}. The OH^- centres are derived from the H_2O solution medium and are incorporated during rapid growth. Lattice distortion by OH incorporation and the breaking of the oxygen bridges may lead to quasi-amorphous domains, as confirmed in the case of amethyst (*Lehmann* and *Bambauer*, 1973).

Luminescence emission in quartz

The luminescence of SiO_2 is generally weak at room temperature, but it is highly variable depending on the specific conditions of silica formation (Fig. 2). Nevertheless, crystalline SiO_2 modifications and amorphous silica show similar main luminescence bands. This is due to the fact, that short-range order defects in

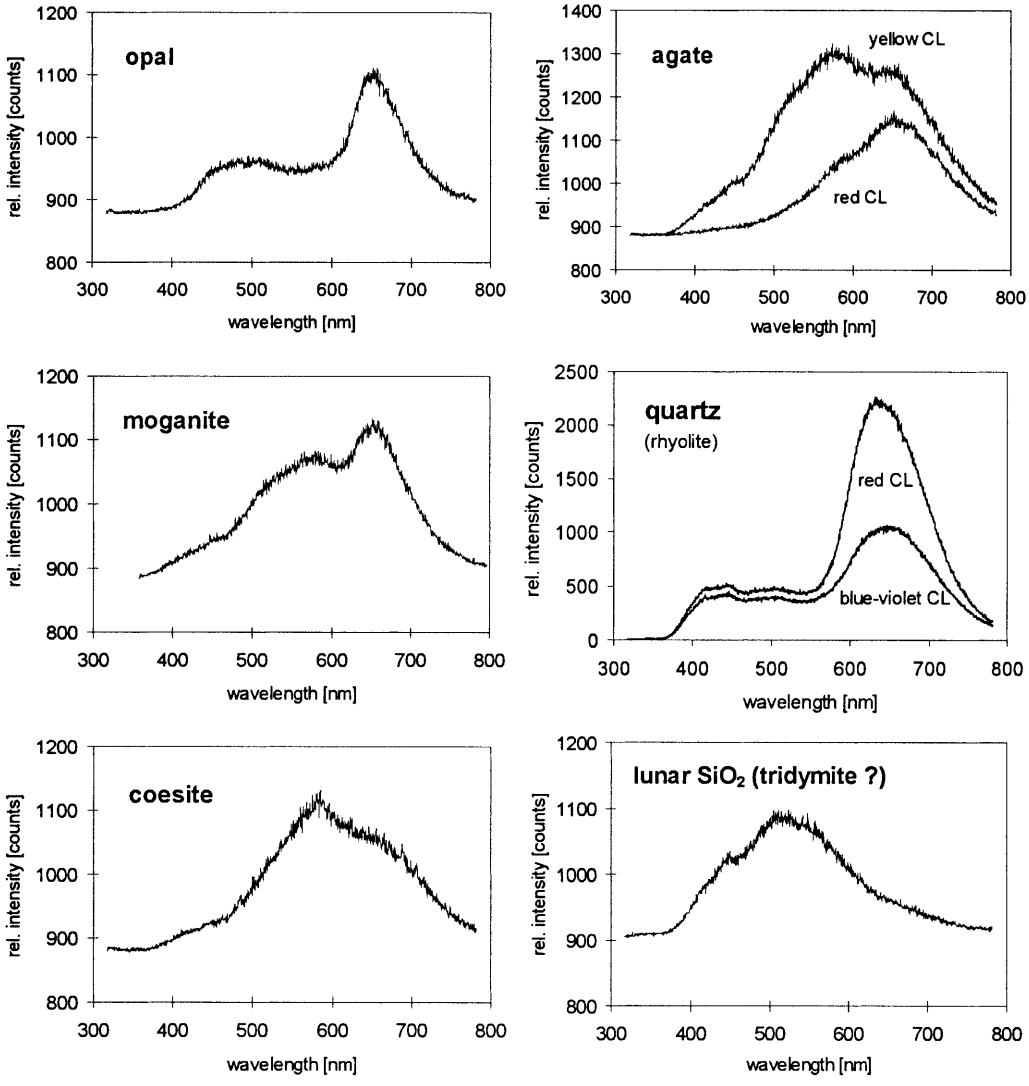

Fig. 2. Typical CL emission spectra of various silica modifications

the silicate structure are determined mainly by silicon-silicon and silicon-oxygen interactions rather than by interactions between oxygen atoms (*Walker*, 1985). Since a strict correlation between the intensities of CL bands and concentrations of specific defects or trace elements does not exist, the interpretation of the origin of luminescence bands in quartz is difficult. Furthermore, the band positions of the luminescence emissions can vary depending on the particular SiO_2 polymorph structure and experimental conditions (e.g., *Luff* and *Townsend*, 1990; *Itoh* et al., 1988). For instance, changes of the cathodoluminescence properties can be detected due to modification of the filling of traps and beam damage such as bond breaking or impurity diffusion (*Remond* et al., 1992). In general, CL emission bands have a Gaussian shape in energy space and broad peak widths (full width at half-maximum, FWHM) greater than 0.15 eV (*Yacobi* and *Holt*, 1990; *Stevens Kalceff* et al., 2000).

Table 1. *Characteristic emission bands in the luminescence spectra of quartz (modified after*, Götze, *1996*; Krbetschek *et al., 1998)*. CL *cathodoluminescence*, TL *thermoluminescence*, PL *photoluminescence*, FWHM *full width at half-maximum (data from* Stevens Kalceff *et al., 2000)*

Emission (FWHM)	Proposed origin	Method	References
175 nm	Intrinsic emission of pure SiO_2	CL	*Entzian* and *Ahlgrimm* (1983)
7.1 eV			
290 nm	Oxygen deficient centre	PL, CL	*Jones* and *Embree* (1976)
4.3 eV	(ODC)	CL	*Skuja* and *Entzian* (1986)
340 nm	Oxygen vacancy	TL	*Rink* et al. (1993)
3.65 eV	$[AlO_4/Li^+]$ centre	CL	*Demars* et al. (1996)
	$[TiO_4/Li^+]$ centre	TL	*Plötze* and *Wolf* (1996)
380–390 nm	$[AlO_4/M^+]$ centre	RL	*Alonso* et al. (1983)
3.1–3.3 eV	$M^+ = Li^+$, Na^+, H^+	CL	*Luff* and *Townsend* (1990)
(0.37 eV)	$[H_3O_4]^0$ hole centre	TL	*Yang* and *McKeever* (1990)
420 nm	Intrinsic emission	CL	*Stevens Kalceff* and *Phillips* (1995)
2.95 eV		CL	*Gorton* et al. (1997)
(0.33 eV)			
450 nm	Intrinsic defect	CL, RL	*Trukhin* and *Plaudis* (1979)
2.8 eV	Self-trapped exciton (STE)	CL	*Walker* (1985), *Itoh* et al. (1988)
(0.35 eV)		CL	*Stevens Kalceff* and *Phillips* (1995)
			Gorton et al. (1997)
500 nm	$[AlO_4]^0$ centre	CL	*Nassau* and *Prescott* (1975)
2.5 eV	Extrinsic emission	RL	*Itoh* et al. (1988)
	$[AlO_4]^0$, $[GeO_4/M^+]^0$ centre	TL	*Rink* et al. (1993)
	$[AlO_4/M^+]$ centre	TL	*Katz* and *Halperin* (1988)
	$M^+ = Li^+$, Na^+, H^+	CL	*Ramseyer* et al. (1990),
			Perny et al. (1992)
580 nm	Oxygen vacancy	TL	*Rink* et al. (1993)
2.1 eV	Self-trapped exciton (STE)	CL	*Stevens Kalceff* and *Phillips* (1995)
	E′ centre	CL	*Götze* et al. (1999)
620–650 nm	Nonbridging oxygen hole centre	PL	*Siegel* and *Marrone* (1981)
1.95–1.91 eV	Oxygen vacancy	CL	*Luff* and *Townsend* (1990)
(0.42/0.20 eV)	NBOHC with several precursors	CL	*Remond* et al. (1992)
	(e.g., hydroxyl group,	CL	*Stevens Kalceff* and *Phillips* (1995)
	peroxy linkage)		
705 nm	Substitutional Fe^{3+}	CL	*Pott* and *McNicol* (1971)
1.75 eV		CL	*Kempe* et al. (1999)

Investigations of natural and synthetic quartz specimens showed various emission bands which were ascribed to many different intrinsic and extrinsic causes (see Table 1). The visible luminescence of natural quartz consists mainly of several emission bands in the blue and red spectral region. Accordingly, the perceived luminescence colours depend on the relative intensities of the dominant peaks.

The blue luminescence band is usually very broad and consists of overlapping component bands, which can be related to different types of centres. *Gorton* et al. (1997) used a phase-tuning technique to separate and identify the lines from

different centres and found four major components of the blue CL emission centered at 390 nm, 420 nm, 450 nm, and 500 nm.

– *390 nm*: The alkali (or hydrogen)- compensated [AlO_4/M^+] centre has been suggested as being responsible for a deep blue emission band with a maximum intensity at $\sim$390 nm. This transient emission is very sensitive to irradiation damage and correlates well with the Al content and the concentration of paramagnetic [AlO_4/M^+] centres (*Alonso* et al., 1983; *Luff* and *Townsend*, 1990; *Perny* et al., 1992; *Gorton* et al., 1997). Therefore, this emission has been attributed to the recombination of a hole trapped adjacent to a substitutional, charge-compensated aluminium-alkali ion center (*Stevens Kalceff* and *Phillips*, 1995). The rapid attenuation of the 390 nm emission under an electron beam results from the dissociation and electromigration of the charge compensating cations out of the interaction volume under the influence of the irradiation induced electrical field. *Gorton* et al. (1997) concluded that the 390 nm band is probably not completely related to aluminium, since they found a reduced 390 nm band even in ultra-pure synthetic quartz.

The transient 380–390 nm CL emission is a common feature of α-quartz crystallized from aqueous solutions (e.g. hydrothermal quartz).

– *420 nm*: The origin of the 420 nm emission band today is thought to be related to an irradiation-produced intrinsic defect although this emission was previously associated with various other defects such as a carbon impurity, an –O–O– type defect or O_2^- defects (*Stevens Kalceff* and *Phillips*, 1995 and references therein). *Rink* et al. (1993) observed the TL emission at 420–435 nm exclusively in igneous quartz of volcanic and granitic origin.

– *450 nm*: Other main luminescence emissions are observed between 440 nm and 500 nm (2.8 and 2.5 eV) in crystalline SiO_2 and between 515 nm and 565 nm (2.4 and 2.2 eV) in amorphous SiO_2 (*Itoh* et al., 1988; *Luff* and *Townsend*, 1990; *Stevens Kalceff* and *Phillips*, 1995). According to *Itoh* et al. (1988) the 2.8 eV emission is intrinsic while the 2.5 eV emission band is extrinsic (impurities).

The 450 nm emission is strongly polarised along the c-axis and is due to the recombination of the so-called self-trapped exciton (*Stevens Kalceff* and *Phillips*, 1995). The self-trapped exciton involves an irradiation-induced electron hole pair (oxygen Frenkel pair consisting of an oxygen vacancy and a peroxy linkage) and is a consequence of the strong electron-phonon interactions in SiO_2 (*Hayes*, 1990). The 450 nm emission is more or less present in all genetic quartz types (compare Fig. 2).

– *500 nm*: The origin of the emission peak at $\sim$500 nm was in discussion during the last decade. *Nassau* and *Prescott* (1975) first associated an $[AlO_4]^0$ centre from a substitutional Al^{3+} with the emission band at 485 nm (2.55 eV). *Itoh* et al. (1988) related the 2.5 eV emission to an extrinsic process due to the substitutional incorporation of impurity ions. *Rink* et al. (1993) reported a narrow, intense 470 nm TL emission in quartz from Li-rich pegmatites which they related to Al and Ge defects. In general, the 500 nm emission is the dominant emission band in pegmatitic quartz of different origin (*Götze*, unpubl. data; Fig. 3).

Ramseyer and *Mullis* (1990) and *Perny* et al. (1992) provided a thorough discussion concerning the short-lived blue-green CL emission band around 500 nm.

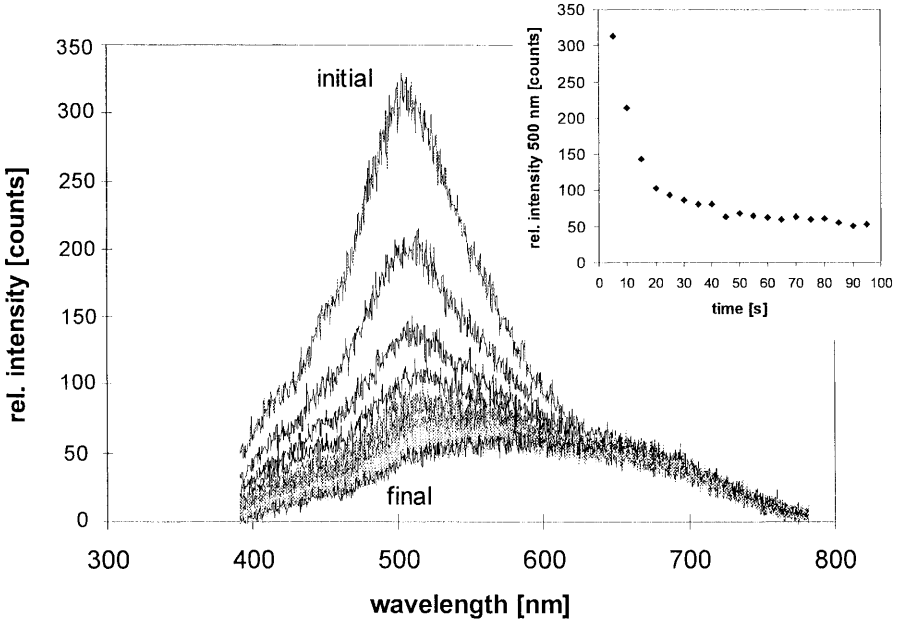

Fig. 3. Time dependent emission spectra of the short-lived blue-green CL of a rose quartz sample, Rubicon Mine (Namibia); the time-scan (20×5 s) illustrates the strong intensity decrease of the 500 nm emission during electron bombardement (compare inset)

CL observations, microprobe analysis, heat- and electrodiffusion experiments revealed that the CL can be related to the uptake of positively charged interstitial cations (H^+, Na^+, Li^+, K^+) associated with the substitution of Al for Si. The highest intensities of the short-lived blue CL emission were detected in zones with Al and Li concentrations of up to 10000 atoms per 10^6 Si (ppma), whereas zones with < 5 ppma Al were nonluminescent (*Perny* et al., 1992).

The intensity of the blue luminescence emission falls off rapidly after electron bombardment within 30 to 60 seconds (Fig. 3). The intensity decrease of the 500 nm emission band during continuous electron bombardment can be related to ionization-enhanced diffusion of luminescence centres as it was shown by *Ramseyer* and *Mullis* (1990) by electrodiffusion studies. The intensity decrease (Fig. 3) can be described by an equation

$$I(t) = I_s + I_{u0} \cdot e^{-k \cdot t},$$

where I_s is the stable component of the 500 nm emission, I_{u0} the initial intensity of the short-lived unstable CL emission, k the decay constant and t the time of electron bombardment. The short-lived CL can be restored by heating the quartz to 500 °C for one day (*Perny* et al., 1992) indicating an opposite mechanism to that of TL. This conclusion is emphasized by the observation by *Ramseyer* and *Mullis* (1990) that growth zones in hydrothermal quartz crystals with an intense smoky colouration show a lower luminescence intensity. Furthermore, both natural and artificial γ-irradiation cause a decrease in the intensity of the short-lived blue CL. This can be explained by the conversion of $[AlO_4/M^+]^0$ luminescence centres into $[AlO_4]^0$ colour centres (*Plötze*, 1995).

Besides the short-lived blue CL emission, which is a common feature of hydrothermal and pegmatitic quartz, a stable 500 nm CL emission can be observed both in igneous quartz and in non-crystalline SiO_2 modifications such as opal (Fig. 2) or silica glass.

Although a correlation of the CL response and the concentration of trace elements has been noted by several authors (e.g., Ti: *Müller* et al., 1999; Al: *Walther* et al., 1996; *Watt* et al., 1997) CL zoning in quartz cannot be simply related to variations of the trace-element concentration. In amorphous SiO_2 samples (e.g. opal, silica glass) a positive correlation between Al content and the intensity of the 500 nm emission band was detected (see Plate 2) suggesting that Al may be a significant factor in CL behaviour of SiO_2. Ion microprobe (SIMS) analysis of volcanic quartz phenocrysts and xenocrysts by *Watt* et al. (1997) also showed that Al contents are higher in areas of bright CL emission but they suggested that other factors (e.g. the effect of growth rate on defect density) may also play a major role in controlling CL intensity.

– *510–570 nm*: The CL emission in the 510–570 nm range of Ge doped synthetic quartz was related by *Luff* and *Townsend* (1990) to the decay of a self-trapped exciton following the Ge bond breaking. *Stevens Kalceff* and *Phillips* (1995) found a CL emission at 540 nm which they relate to the radiative recombination of a self-trapped exciton from amorphous SiO_2 outgrowth. In natural quartz samples this CL emission is rarely observed.

– *580 nm*: A broad luminescence emission band centered at 560–580 nm was observed by *Rink* et al. (1993) by TL only in natural quartz of hydrothermal origin and was related to oxygen vacancies. *Stevens Kalceff* and *Phillips* (1995) and *Itoh* et al. (1988) found CL emission bands between 2.1 and 2.4 eV (520–590 nm) in irradiated samples of amorphous SiO_2 and alpha-quartz which they related to the self-trapped exciton. *Götze* et al. (1999) detected the yellow CL emission predominantly in agates and hydrothermal vein quartz of acidic volcanics (Fig. 2 and Plate 1). Since those quartz samples also have the highest content of lattice defects (especially high concentration of oxygen vacancies, i.e. E_1' centres), these defects may be responsible for the yellow CL emission band at 580 nm. The common occurrence of the 580 nm emission band in cryptocrystalline quartz can possibly be related to rapid growth probably from a noncrystalline precursor.

– *620–650 nm*: The orange to red emission band at about 620–650 nm has been detected in almost all synthetic and natural quartzes with most intense emissions in hydrothermal and cryptocrystalline quartz (*Götze* et al., 1999). This emission is attributed to the recombination of electrons in the nonbridging oxygen band-gap state with holes in the valence-band edge (*Siegel* and *Marrone*, 1981). A number of different precursors of this nonbridging oxygen hole center have been proposed such as hydrogen or sodium impurities, peroxy linkages (oxygen-rich samples), or strained silicon-oxygen bonds, which may influence the band position (*Stevens Kalceff* and *Phillips*, 1995). Therefore, at least two overlapping band positions at 620 nm (1.95 eV) and 650 nm (1.91 eV) may be distinguished.

Stevens Kalceff et al. (2000) concluded that the 1.95 eV (620 nm) CL component related to the nonbridging oxygen hole centre (NBOHC) with nonbridging hydroxyl

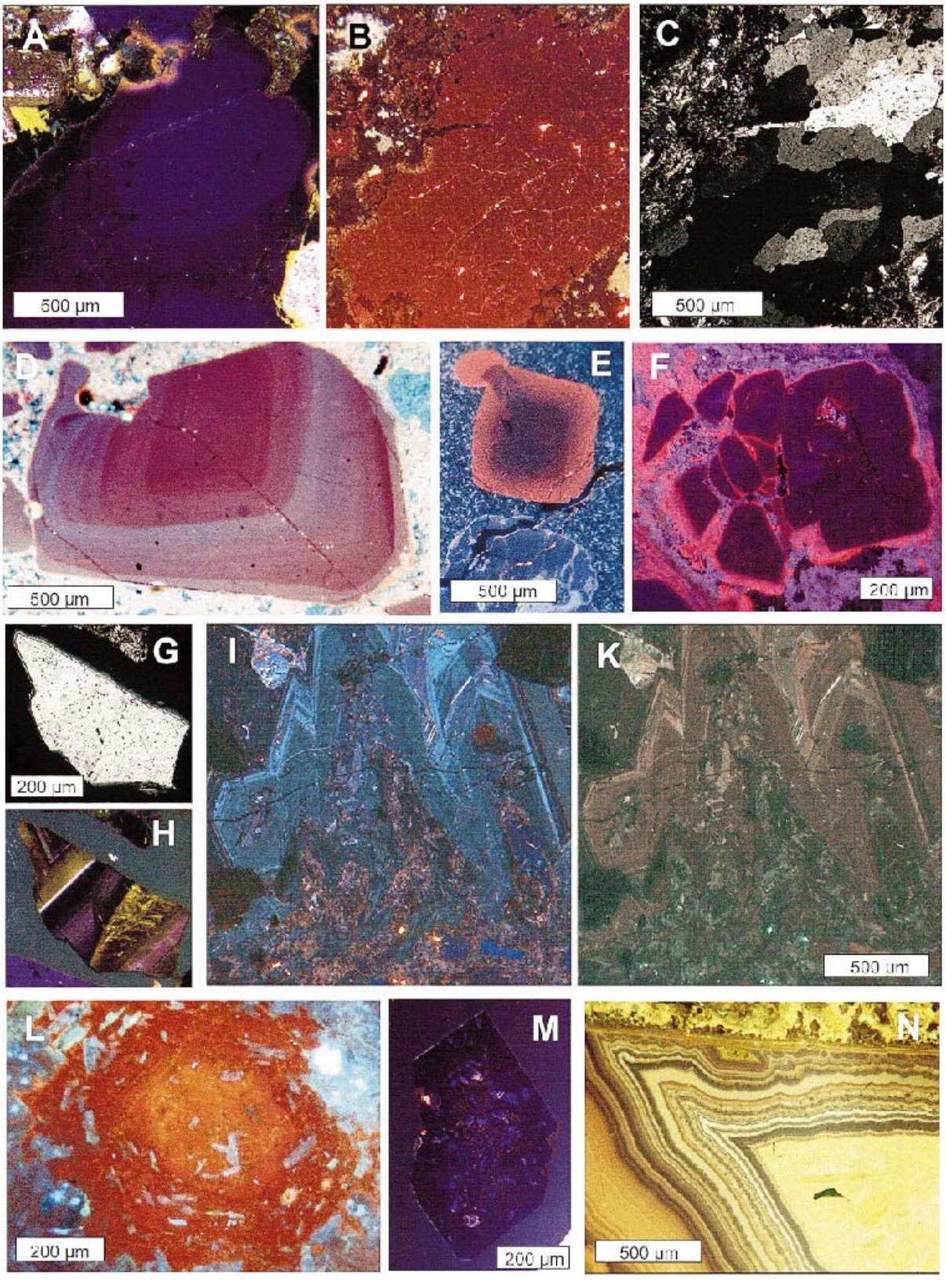
A
500 µm
B
C
500 µm
D
500 µm
E
500 µm
F
200 µm
G
200 µm
H
I
K
500 µm
L
200 µm
M
200 µm
N
500 µm

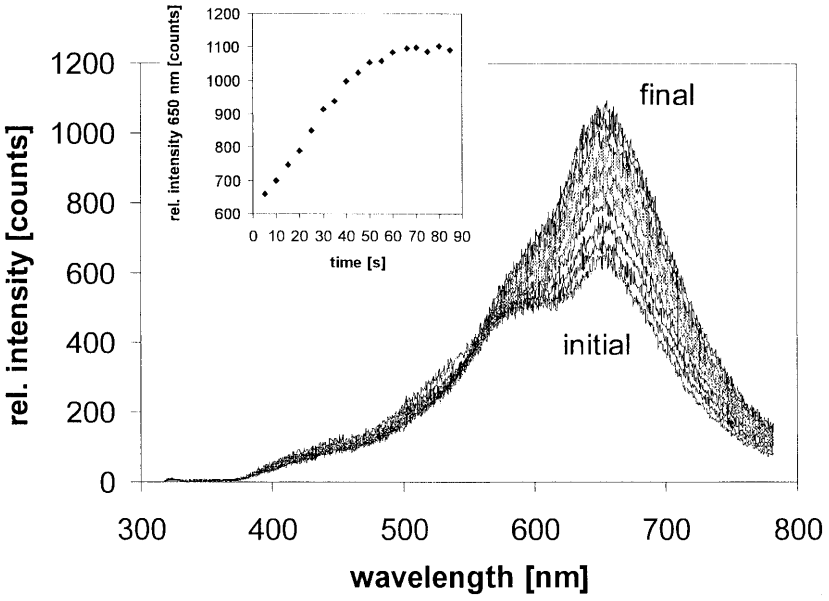

Fig. 4. Time dependent CL spectra of an agate sample from Frydstejn, Bohemia (data from *Götze* et al., 1999); the time-scan illustrates the strong intensity increase of the 650 nm emission during electron bombardement (compare inset)

precursors (≡Si–OH) is rapidly attenuated by electron irradiation. In natural SiO_2 samples the 620 nm emission was especially detected in authigenic quartz of sedimentary origin and silicified wood. The CL emission at 1.91 eV (650 nm) initially increases during electron bombardement due to the formation of non-bridging oxygen cetres from the precursors and then stabilizes (Fig. 4). Comparative studies

Plate 1. CL micrographs of quartz samples from different parent rocks with typical CL behaviour. **A** Blue-violet luminescing quartz from Königshain granite, Lusatia (Germany); **B/C** CL (**B**) and crossed polars (**C**) images of a brown luminescing polycrystalline metamorphic quartz from a schist (Erzgebirge, Germany); **D** Rhyolitic quartz grain from Euba, Germany showing distinct oscillatory zoning which is only visible under CL; **E** Quartz phenocryst within the rhyolite from Thunder Egg, Canada showing a blue luminescing core and a reddish luminescing rim (compare CL spectra in Fig. 2); **F** Broken quartz grain in a rhyolite sample from Rochlitz, Germany showing typical bright reddish luminescing reaction rims; **G/H** A sample of hydrothermal quartz imaged by polarizing microscopy (**G**) and by CL microscopy (**H**) illustrating that CL reveals internal structures and growth zoning which are not discernible by conventional polarizing microscopy; **I/K** Hydrothermal quartz from Ehrenfriedersdorf, Germany showing initial short-lived blue CL (**I**) changing to brown CL during electron bombardement (**K**) (explanation see text and Fig. 6); **L** Quartz with snow-ball structure (intergrown with albite) from Nuweibi, Egypt; **M** Hypidiomorphic authigenic quartz grown in a sulfate-rich environment from the salt deposit Roßleben, Germany; note the numerous anhydrite inclusions visible by blue CL; **N** Agate sample with quartz incrustation in a rhyolite from Chemnitz, Germany showing a typical yellow luminescence colour (from *Götze* et al., 1999; compare CL spectrum in Fig. 2)

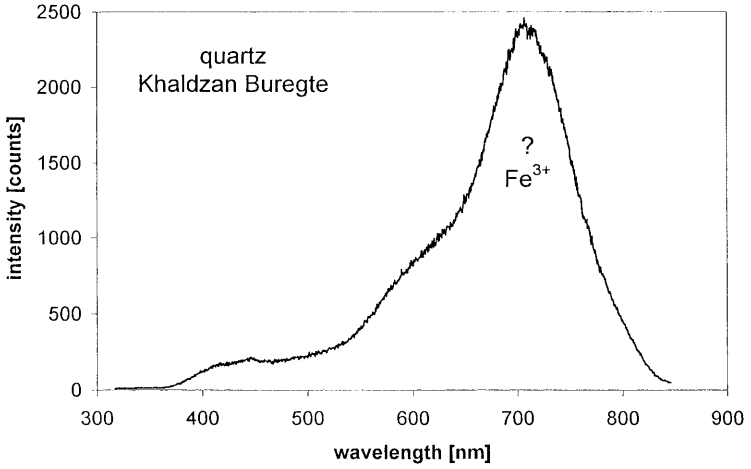

Fig. 5. CL emission spectrum of quartz from Khaldzan Buregte, Mongolia (compare Plate 2A) showing a strong emission band at 705 nm probably due to Fe^{3+}

on radiation damaged and undamaged quartz samples have shown that a final stage of lattice damage, i.e. a maximum intensity of the 650 nm emission can be reached in radiation damaged quartz (*Habermann* et al., 1997).

Götze et al. (1999) concluded that high intensities of the 650 nm emission in agate can probably be assigned to high concentration of O_2^{3-} centres which are formed by irradiation. Silanol groups, which are a constituent of the agate structure (*Flörke* et al., 1982), are the favourable precursors of these non-bridging oxygen centres. A correlation of the abundance of OH related defects in quartz and the intensity of the 650 nm emission was also reported from metamorphic quartz (*Behr* et al., 1989) and igneous quartz (*Müller* et al., 1999).

– *705 nm*: The emission in the red on the edge to the IR around 705 nm is assumed to be due to the substitutional incorporation of Fe^{3+} into the quartz lattice like in other silicates (*Pott* and *McNicol*, 1971; *Gorobets* et al., 1989; *Kempe* et al., 1999). *Pott* and *McNicol* reported this red/IR emission for the first time from synthetic quartz crystals. Recently, some red luminescing quartz was found in metasomatically overprinted granites from Khaldzan Buregte, Mongolia (*Kempe* et al., 1999). The CL spectra show a strong emission band at $\sim$705 nm which can probably be attributed to the incorporation of Fe^{3+} into the quartz lattice (Fig. 5 and Plate 2A). The ferric iron results from fenitization processes within the granite massif and was also detectable in other minerals such as albite, zircon or fluorite. However, the origin of the 705 nm emission has to be further verified by measurements of the luminescence lifetime and/or the luminescence excitation spectrum.

– *UV*: Additional luminescence emissions have been observed in the UV region of the spectrum. The emission bands at 175 nm, at 290 nm and at 340 nm have been generally related to intrinsic defects (*Jones* and *Embree*, 1976; *Entzian* and *Ahlgrimm*, 1983; *Rink* et al., 1992). Furthermore, *Demars* et al. (1996) found an

additional strong correlation of the Al and Li contents with the CL emission band at 330–340 nm indicating that [AlO_4/Li^+] centres may also serve as activators for this UV emission. *Plötze* and *Wolf* (1996) concluded from results of TL and EPR measurements that [TiO_4/Li^+] centres may serve as activators and vacancy centres as recombination sites for the 340 nm emission.

Applications of quartz CL

Though a considerable number of research on luminescence is empirical, a wealth of information can be obtained on descriptive features and typomorphic criteria. The weak but highly variable CL colours and emission spectra of quartz can be related to genetic conditions of quartz formation. Hence, both luminescence microscopy and spectroscopy have been used widely in various typomorphic quartz studies.

One of the most important fields of application of quartz CL is the possibility to reveal internal structures, growth zoning and lattice defects in quartz crystals not discernible by means of other analytical techniques (e.g. plate 1G/H). During both quartz crystallization from the melt and from solutions, variations of the physico-chemical conditions result in crystal zoning (Plates 1 and 2). This enables to reconstruct the specific growth conditions or to reveal multiphase processes. The zoning in quartz can be related either to variations in trace-element uptake (charge balancing single charged cations associated with the substitution of Al for Si) or to intrinsic defects caused by effects of the growth conditions. *Ramseyer* and *Mullis* (1990) and *Perny* et al. (1992) explained the variations of the trace-element concentration at a microscopic scale in hydrothermal quartz particularly by changes in pH. Another important property of quartz is the variability of its CL colour in dependence on the specific origin. *Zinkernagel* (1978) established one of the first classification schemes of quartz CL colours in sandstones. He divided the CL phenomena into three groups: (I) ''violet'' or blue luminescing quartz (major peaks at 450 nm and 620 nm) derived from igneous and high-grade metamorphic rocks which have undergone relative fast cooling, (II) ''brown'' luminescing quartz (major peak around 620 nm and a minor near 450 nm) from low-grade metamorphic rocks or slowly cooled high-grade metamorphic rocks and (III) non-luminescing quartz of authigenic (sedimentary) or hydrothermal origin.

However, numerous investigations of a wide spectrum of quartz-bearing rocks show that a principal genetic correlation of quartz particles based upon their CL properties is not possible in every case, because quartz grains with similar CL colours and emission spectra, respectively, may have grown under different genetic conditions. Nevertheless, a general classification is often used as first based interpretation including the following CL colour shades of quartz (e.g., *Ramseyer* et al., 1988; *Götze*, 1996 – compare plates 1 and 2): (i) *blue to violet*: plutonic quartz as well as quartz phenocrysts in volcanic rocks, and high-grade metamorphic quartz (Plate 1A), (ii) *red*: matrix quartz and quartz phenocrysts in volcanic rocks (Plate 1E), (iii) *brown*: quartz from regional metamorphic rocks (Plate 1B/C), (iv) *non or weakly luminescent*: authigenic quartz (Plate 1M, 2D), (v) *short-lived blue-green*: hydrothermal and pegmatitic quartz (Plate 1I/K).

This general classification can be specified by some detailed observations. For instance, quartz from extrusive igneous rocks commonly luminesces brighter blue

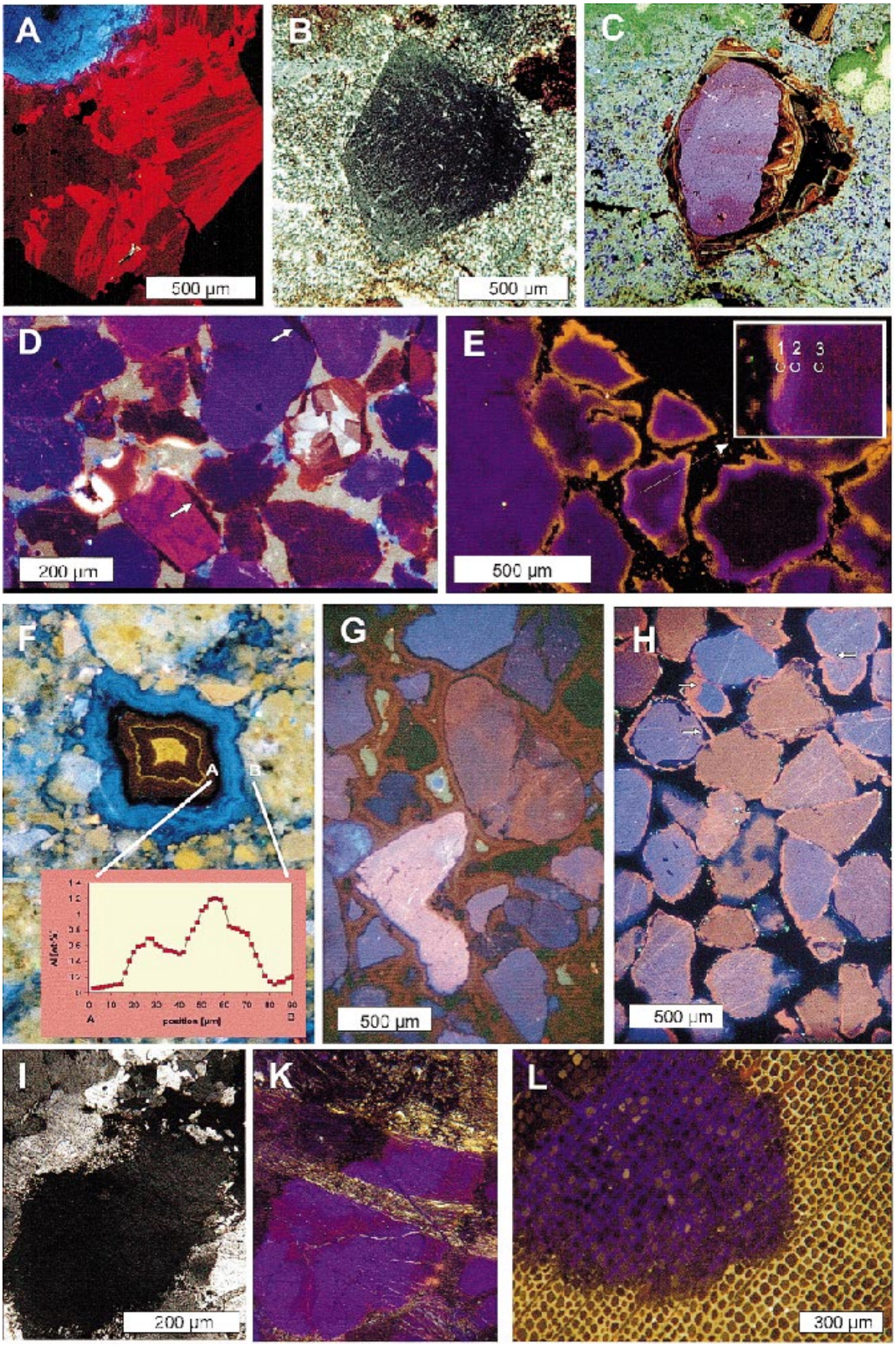
A
500 µm
B
500 µm
C
D
200 µm
E
1 2 3
500 µm
F
A
B
Al [at-%]
position [µm]
G
500 µm
H
500 µm
I
200 µm
K
L
300 µm

than quartz from intrusive rocks. Some extrusive igneous quartz crystals display concentric zoning under CL visible by variations in shade of blue to violet CL (Plate 1D). Spectral analysis of the different luminescing zones has revealed that the variations in CL colour are caused by variations of the intensity ratio of the blue and red CL emission (compare Fig. 2). Spatially resolved trace-element analysis indicate a relationship to the Al content of the different zones (*Schneider*, 1993; *Watt* et al., 1997; *Müller* et al., 1999) induced by varying trace-element uptake during crystal growth. Observed colour-centre zoning in volcanic quartz crystals (*Ritter* and *Dennen*, 1964) would confirm the role of Al ($[AlO_4]^0$ centre) for CL variations at least for the blue emission component. The red component of the CL emission, which often dominates in rims and cracks of the quartz phenocrysts (Plate 1E,F) is more likely related to lattice defects (650 nm emission due to non-bridging oxygen).

Metamorphic quartz that recrystallised at high temperatures (e.g. granulite) reverts to a blue luminescence colour comparable to that of plutonic quartz. Similar observations were made by *Sprunt* et al. (1978) who assumed a relationship between CL colour of quartz and metamorphic grade of naturally deformed quartzites. The originally different CL colours change toward a uniform brownish-red colour through high-grade levels of metamorphism (Plate 1B). *Owen* (1984) speculated that quartz CL turns to a uniform reddish-brown colour above the garnet zone within high-grade metamorphism.

Plate 2. CL micrographs of quartz and rock samples showing typical CL features. **A** Intergrowth of deep red luminescing quartz and albite as well as alkali feldspar; the red CL is activated by Fe^{3+} (compare CL spectrum in Fig. 5), which is incorporated during fenitization processes; **B/C** crossed polars/CL images of a rhyolitic quartz grain from Augustusburg, Germany (from *Götze*, 1996); CL reveals a primary nuclei and alteration by dissolution and hydrothermal crystallization of a secondary quartz generation; **D** CL image of a sandstone sample consisting of detrital quartz grains of different origin (blue-violet = igneous quartz, brown = metamorphic quartz, greenish-brown with zonation = hydrothermal vein quartz); secondarily formed authigenic quartz rims do not luminesce (see arrows); yellow halos are due to radiation damage (modified after *Götze*, 1996); **E** Quartz conglomerate sample from Witwatersrand, South Africa; CL reveals bright luminescing zoned radiation halos on detrital quartz grains caused by migrating uranium bearing fluids; the CL spectra of the different zones (see inset) are documented in Fig. 7; **F** Silcrete sample from Coober Pedy, Australia showing zoned SiO_2 cement (opal); variations in the blue CL are caused by varying Al contents (see inset); **G** Sample of a Tertiary quartzite (silcrete) from Profen, Germany; the detrital quartz grains are clearly distinguishable from brown luminescent cement (chalcedony) and greenish pore space (from *Walther* et al., 1996); **H** Silicified quartz sand sample from Hohenbocka, Germany showing at least three zones of authigenic quartz overgrowths (see arrows): nonluminescent, reddish and orange rims; **I/K** Devonian sandstone sample from the Erzgebirge, Germany imaged by polarizing microscopy (**I**) and CL microscopy (**K**) with secondary hydrothermal overprint, which is only visible under CL due to yellow luminescing fluid trails; **L** CL image of yellowish luminescing silicified wood with well preserved cell structures; the infiltration of a secondary fluid is visible by contrasting blue CL (from *Götze* and *Rößler*, 2000)

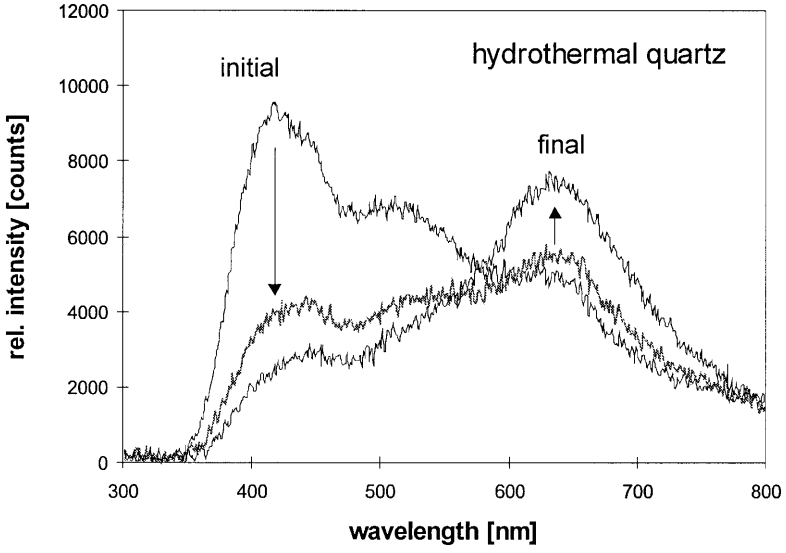

Fig. 6. Time dependent CL emission spectra (3 × 20 s) of a synthetic hydrothermal quartz sample; the initially strong emission bands around 400 nm and at 500 nm rapidly decrease, whereas the 650 nm emission increases resulting in a change of the visible CL colour from blue to brown (note that the detector characteristics prevent quantitative measurements below 380 nm)

The brown and reddish-brown CL colours (emission band at 620–650 nm) can also be explained by lattice defects induced by twinning, mechanical deformation, particle bombardment or rapid growth (*Ramseyer* et al., 1988). For instance, quartz from granitic rocks of the Siljan impact structure (Sweden) exhibits reddish CL colour, presumably induced by the shock-heating episode of the impact and by a subsequent temperature rise in the granite (*Ramseyer* et al., 1992). Similar conclusions were drawn for shocked quartz from lunar soil (*Sippel* and *Spencer*, 1970) and terrestrial occurrences (*Serebrennikov* et al., 1982) or quartz from a Cretaceous/Tertiary boundary impact (*Owen* and *Anders*, 1988).

Another conspicuous feature of quartz CL is the short-lived bottle-green or blue CL in α-quartz which is typical of quartz crystallized from hydrothermal solutions. The typical change from initial blue to final brown CL colours (see Plate 1I/K) is caused by the rapid decrease of the CL emission bands just below 400 nm and at 500 nm and the increase of the red emission band (compare Fig. 6). This characteristic transient CL behaviour was observed both in natural and synthetic hydrothermal quartz specimens.

In contrast, most quartz crystals formed under high-temperature conditions from a melt show a stable luminescence behaviour. This property may serve to rapidly distinguish quartz crystallized from a solution from that crystallized from a melt. Plate 2B/C, for instance, shows a quartz phenocryst from the Augustusburg rhyolite, Saxony under crossed polars and CL. Whereas polarizing microscopy could not discerne any alteration, CL reveals quartz dissolution (primary quartz) and secondary hydrothermal quartz formation by silica-bearing fluids during rhyolite alteration.

The diversity of CL colours in quartz in dependence on its origin permits the recognition of specific physico-chemical condition of formation. Detrital quartz of sediments, for instance, provides the basis for provenance studies assuming that the CL colour of the clastic quartz grains remained unchanged from its original source rock (Plate 2D). Over the past decades a considerable number of such provenance studies has been published based on the CL behaviour of quartz (e.g. *Zinkernagel*, 1978; *Füchtbauer* et al., 1982; *Matter* and *Ramseyer*, 1985; *Owen*, 1991; *Götze* and *Blankenburg*, 1992; *Seyedolali* et al., 1997; *Götze*, 1998). Because of the insufficiency of a quartz classification based solely on CL colours it is necessary to combine CL provenance studies with other analytical methods such as trace-element analysis, isotope studies or inclusion studies (*Götze* and *Zimmerle*, 2000).

Cathodoluminescence also strongly assists in the reconstruction of diagenetic processes since CL allows to discriminate between detrital quartz grains and their overgrown cement. Secondary overgrowths, ghosts of the original fabric, evidence of pressure solution as well as fracturing and healing phenomena are more clearly revealed by CL than by conventional microscopy. Especially when dust rims are absent in sandstones, cathodoluminescence reveals detrital nuclei and optically continuous quartz overgrowth (Plate 2G/H) and permits a quantification of quartz cements by means of combined CL and image analysis (*Evans* et al., 1994; *Götze* and *Magnus*, 1997). Such observations are important to discern various geological and mineralogical aspects, particularly in the field of oil exploration (e.g. *Houseknecht*, 1991).

The previously assumed non-luminescent character of authigenic quartz overgrowths seems to be less common than suggested in earlier investigations. Although secondary quartz rims often show lower CL intensities than detrital grains, modern CL equipments revealed quartz overgrowths with stable reddish-brown and blue as well as short-lived blue-green and yellow luminescence colours (e.g. *Burley* et al., 1989; *Neuser* et al., 1989; *Ramseyer* and *Mullis*, 1990; *Morad* et al., 1991; *Götze* and *Walther*, 1995; *Bruhn* et al., 1996). Moreover, *Demars* et al. (1996) detected a CL emission band in authigenic quartz overgrowths outside the visible region around 340 nm in the UV. The stable luminescence is in general interpreted as to result from the burial diagenetic conditions, whereas the short-lived CL was more related to hot basinal brines or hydrothermal solutions.

The application of CL and a careful evaluation and description of the microscopic CL phenomena and patterns best revealed detailed aspects of quartz cementation, silicification, and grain dissolution: e.g. quartzitic fabric with triple junctions of grain boundaries, two-phase quartz cementation, evidence of a first dissolution event, and the presence of pressolved grain contacts between stacked quartz grains. In detailed mineralogical and geochemical studies on Australian and German silcretes *Walther* and *Götze* (1993), *Götze* and *Walther* (1995) and *Walther* et al. (1996) applied CL to distinguish several types of silica cement (opal, chalcedony, quartz) not discernible by polarizing microscopy alone. Corroded clastic quartz grains and multiphase cement generations reflect changes in physico-chemical conditions during quartz precipitation (Plate 2F–H).

In a similar way, CL can be used to unravel deformation features or fluid migration pathways in crystalline as well as in sedimentary rocks. *Millikan* and

Laubach (2000), for instance, demonstrated that CL is an excellent tool to distinguish brittle or ductile deformation processes during sandstone diagenesis. On the other hand, CL can reveal fluid migration due to hydrothermal alteration or pro- and retrograde metamorphic conditions which is often not recognized by conventional polarizing microscopy (e.g., *Behr*, 1989; *Frentzel-Beyme*, 1989; *Van den Kerkhoff* and *Müller*, 1999). Plate 2K shows an example of different fluid generations within a Devonian sandstone sample from the Erzgebirge, Germany. The causes of the CL contrast between fluid migration paths and the host crystals are recrystallization and/or deformation processes caused by the diffusion of the fluids. Plate 2L depicts the infiltration of a secondary fluid (blue CL colour) into the well preserved cell structure of silicified wood (yellow CL). CL clearly reveals the secondary process because of the drastic change in the luminescence behaviour of the altered area.

Lattice damages due to alpha radiation in quartz can also be visualised by cathodoluminescence. Such lattice damages cause halos around uranium and thorium-bearing accessory minerals (e.g. zircon), which are much larger than the mineral inclusions themselves (*Owen*, 1988; *Meunier* et al., 1988; *Ramseyer* et al., 1988; *Götze*, 1996). But also pores, and recent and previous migration tracks of uranium bearing fluids can be depicted by their radiation rims in quartz of sandstones and crystalline rocks. Plate 2E shows quartz grains from the Witwatersrand conglomerate characterized by three concentric radiation-damage rims. These rims are due to alpha particles, which create lattice damage when penetrating the quartz. Figure 7 illustrates that the radiation halos are characterized by a strong increase of the 650 nm CL emission band (nonbridging oxygen hole centre), visible by violet and orange CL colours, respectively. These nonbridging oxygens are probably caused by bond breaking due to the alpha particles. The width of the differently luminescing rims (16, 24 and 37 μm) can be related to the energies of the alpha

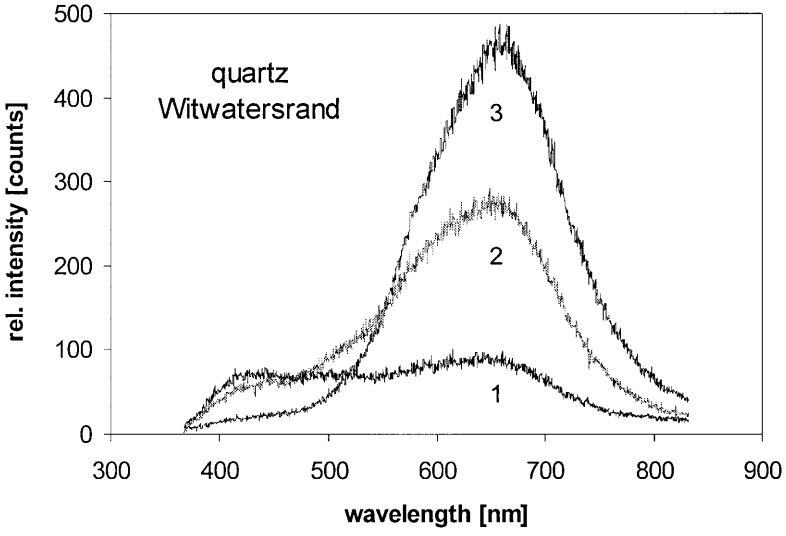

Fig. 7. CL emission spectra of the blue luminescing detrital core (1) of a quartz grain within the Witwatersrand quartz conglomerate (see plate 2E), and the violet (2) and orange (3) radiation halos, respectively (explanation see text)

particles from the ^{238}U decay series according to the Bragg-Kleeman rule (*Owen*, 1988).

First attempts were also made to use the CL behaviour of quartz in technical processes. In a study of the melting behaviour of quartz raw materials, the quartz material of different origin was quantified using CL and correlated with the melting kinetics (*Götze* et al., 1993). CL is also a useful tool for investigations of the chemical composition and structure of certain silicate glasses and fused silica. Especially variations of the chemical composition (e.g. Al content), inclusions or streaks are visible as heterogeneities under the CL (*Götze*, 1996). Furthermore, intrinsic defects in high-purity glassy SiO_2 and SiO_2 films for high-tech applications can be detected by CL studies (e.g., *Skuja* and *Entzian*, 1986).

Conclusions

The present study summarizes results of extensive cathodoluminescence studies on quartz of different origin. The presented data emphasize the advantages and great potentials of CL in several fields of quartz research. CL can be used in a purely descriptive way to detect quartz of different origin or to reveal processes of crystal growth, recrystallization, alteration or diagenesis by variable CL colours. On the other hand, CL is an effective method for spatially resolved analysis of point defects in quartz by spectral measurements. In combination with EPR measurements and spatially resolved trace-element analysis the different emission bands can be related to specific lattice defects in the quartz structure. The defects causing different CL emissions often reflect the specific physico-chemical conditions of crystal growth and therefore, can be used as a signature of genetic conditions. In conclusion, the application of CL microscopy and spectroscopy has a great potential for a multitude of quartz studies in science and technology, especially in combination with other spatially resolved analytical methods.

Acknowledgements

Parts of this research were funded by the Deutsche Forschungsgemeinschaft (DFG-grants Bl 315/1 and Go 677/1), which we gratefully acknowledge. Reviews by *K. Ramseyer* and two anonymous reviewers led to significant improvements of the manuscript.

References

Agel A (1992) Paramagnetische Defektzentren in polykristallinem Quarz granitischer und metamorpher Herkunft. Thesis, University of Marburg, 109 p (unpublished)

Alonso PJ, Halliburton LE, Kohnke EE, Bossoli RB (1983) X-ray induced luminescence in crystalline SiO_2. J Appl Phys 54: 5369–5375

Baker JM, Robinson PT (1983) EPR of a new defect in natural quartz: possibly O_2^-. Solid State Comm 48: 551–556

Bambauer HU (1961) Spurenelementgehalte und Farbzentren in Quarzen aus Zerrklüften der Schweizer Alpen. Schweiz Miner Petrol Mitt 41: 335–369

Behr HJ (1989) Die geologische Aktivität von Krustenfluiden. Niedersächs Akad Geowiss Veröff H 1: 7–41

Behr HJ, Neuser RD, Schmidt-Mumm A, Schneider N (1989) Untersuchungen zur Kathodolumineszenz, Infrarotspektroskopie und Dekripitometrie am Bohrprofil der KTB-Vorbohrung. KTB-Report 89-3: 452

Blankenburg H-J, Götze J, Schulz H (1994) Quarzrohstoffe. Dtsch Verl Grundstoffind mbH, Leipzig-Stuttgart, 296 p

Bruhn F, Bruckschen P, Meijer J, Stephan A, Richter DK, Veizer J (1996) Cathodoluminescence investigations and trace-element analysis of quartz by micro-PIXE: implications for diagenetic and provenance studies in sandstone. Can Mineral 34: 1223–1232

Burley SD, Mullis J, Matter A (1989) Timing diagenesis in the Tartan reservoir (UK North Sea): constraints from cathodoluminescence microscopy and fluid inclusion studies. Mar Petrol Geol 6: 98–120

Demars C, Pagel M, Deloule E, Blanc P (1996) Cathodoluminescence of quartz from sandstones: interpretation of the UV range by determination of trace element distributions and fluid-inclusion P-T-X properties in authigenic quartz. Am Mineral 81: 891–901

Entzian W, Ahlgrimm C (1983) Vergleichende Untersuchungen zur Kathodolumineszenz von SiO_2. Wiss Z W-Pieck-Univ Rostock, Naturwiss Reihe 32: 27–29

Evans J, Hogg AJC, Hopkins MS, Howarth RJ (1994) Quantification of quartz cements using combined SEM, CL, and image analysis. J Sed Res A64: 334–338

Flörke OW, Köhler-Herbertz B, Langer K, Tönges I (1982) Water in microcrystalline quartz of volcanic origin: agates. Contrib Mineral Petrol 80: 324–333

Frentzel-Beyme K (1989) REM-Kathodolumineszenz-Strukturen im Quarzteilgefüge von Metamorphiten: Bestandsaufnahme und geologische Interpretation. Thesis, University of Göttingen

Friebele EJ, Griscom DL, Stapelbroek M, Weeks RA (1979) Fundamental defect centers in glass: the peroxy radical in irradiated, high-purity, fused silica. Phys Rev Lett 42: 1346–1348

Füchtbauer H, Leggewie R, Gockeln C, Heinemann C, Schröder P (1982) Methoden der Quarzuntersuchung, angewandt auf mesozoische und pleistozäne Sandsteine und Sande. N Jb Geol Paläont Mh: 193–210

Gorobets BS, Gaft ML, Podolskyi AM (1989) Luminescence of minerals and ores (in Russ). Ministery of Geology, Moscow, 53 p

Gorton NT, Walker G, Burley SD (1996) Experimental analysis of the composite blue CL emission in quartz. J Lumin 72–74: 669–671

Götze J (1996) Kathodolumineszenz von Quarz – Grundlagen und Anwendung in den Geowissenschaften. Aufschluß 47: 145–164

Götze J (1998) Geochemistry and provenance of the Altendorf feldspathic sandstone in the Middle Bunter of the Thuringian basin (Germany). Chem Geol 150: 43–61

Götze J, Blankenburg H-J (1992) The genesis of the Hohenbocka quartz sand (Eastern Germany) – new results of mineralogical and geochemical investigations. N Jb Geol Paläont Teil I: 1217–1231

Götze J, Magnus M (1997) Quantitative determination of mineral abundance in geological samples using combined cathodoluminescence microscopy and image analysis. Eur J Mineral 9: 1207–1215

Götze J, Plötze M (1997) Investigation of trace-element distribution in detrital quartz by Electron Paramagnetic Resonance (EPR). Eur J Mineral 9: 529–537

Götze J, Rößler R (2000) Kathodolumineszenz-Untersuchungen an Kieselhölzern. I. Silifizierungen aus dem versteinerten Wald von Chemnitz (Perm, Deutschland). Veröff Museum Naturkunde Chemnitz 23: 35–50

Götze J, Walther H (1995) A complex mineralogical and geochemical study on a silicified Miocene quartz sand. Zbl Geol Paläont Teil I H 1/2: 119–129

Götze J, Zimmerle W (2000) Quartz and silica as guide to provenance in sediments and sedimentary rocks. E Schweizerbart'sche Verlagsbuchhandlung, Stuttgart, 91p (Contrib Sediment Geol 21)

Götze J, Höhne D, Do TQ (1993) Genesis and melting behavior of quartz raw materials. Sprechsaal Intern Ceramics & Glass Mag 126: 473–478

Götze J, Plötze M, Fuchs H, Habermann D (1999) Defect structure and luminescence behaviour of agate – results of electron paramagnetic resonance (EPR) and cathodoluminescence (CL) studies. Mineral Mag 63: 149–163

Griffiths JHE, Owen J, Ward IM (1954) Paramagnetic resonance in neutron-irradiated diamond and smoky quartz. Nature 173: 439–442

Griscom DL (1985) Defect structure of glasses: some outstanding questions in regard to vitreous silica. J Non-Cryst Sol 73: 51–77

Habermann D, Götze J, Neuser RD, Richter DK (1997) The phenomenon of intrinsic cathodoluminescence: case studies of quartz, calcite and apatite. Zbl Geol Paläont Teil 1 H 10–12: 1275–1284

Halliburton LE, Jani MG, Bossoli RB (1984) Electron spin resonance and optical studies of oxygen vacancy centers in quartz. Nucl Instr Meth Phys Res B1: 192–197

Hayes W (1990) The structure of the self-trapped exciton in quartz. Rev Solid State Sci 4: 543–546

Houseknecht DW (1991) Use of cathodoluminescence petrography for understanding compaction, quartz cementation, and porosity in sandstones. In: *Barker CE*, *Kopp OC* (eds) Luminescence microscopy: quantitative and qualitative aspects. SEPM, Dallas/ Texas, pp 59–66

Itoh C, Tanimura K, Itoh N (1988) Optical studies of self-trapped excitons in SiO_2. J Phys C, Solid State Phys 21: 4693–4702

Jani MG, Bossoli RB, Halliburton LE (1983) Further characterization of the E_1' center in crystalline SiO_2. Phys Rev B27: 2285–2293

Jones CE, Embree D (1976) Correlations of the 4.77–4.28 eV luminescence band in silicon dioxide with oxygen vacancy. J Appl Phys 47: 5365–5371

Katz S, Halperin A (1988) The low temperature phosphorescence and thermoluminescence of quartz crystals. J Lumin 39: 137–143

Kempe U, Götze J, Dandar S, Habermann D (1999) Magmatic and metasomatic processes during formation of the Nb-Zr-REE deposits from Khaldzan Buregte (Mongolian Altai): indications from a combined CL – SEM study. Mineral Mag 63: 165–167

Kostov RI, Bershov LV (1987) Systematics of paramagnetic electron-hole centers in natural quartz (in Russ). Izvest AN SSSR, ser geol 7: 80–87

Krbetschek MR, Götze J, Dietrich A, Trautmann T (1998) Spectral information from minerals relevant for luminescence dating. Radiat Meas 27: 695–748

Lehmann G, Bambauer HU (1973) Quarzkristalle und ihre Farbe. Ang Chemie 85: 281–289

Luff BJ, Townsend PD (1990) Cathodoluminescence of synthetic quartz. J Phys Condens Matter 2: 8089–8097

Marfunin AS (1979) Spectroscopy, luminescence and radiation centres in minerals. Springer, Berlin Heidelberg New York, 352 p

Matter A, Ramseyer K (1985) Cathodoluminescence microscopy as a tool for provenance studies of sandstones. In: *Zuffa GG* (ed) Provenance of arenites. D Reidel, Boston, pp 191–211 (NATO ASI series C 148)

McKeever SWS (1984) Thermoluminescence in quartz and silica. Radiat Prot Dos 8: 81–98

Medlin WL (1962) Thermoluminescence in quartz. J Chem Phys 38: 1132–1143

Meunier JD, Sellier E, Pagel M (1990) Radiation-damage rims in quartz from uranium-bearing sandstones. J Sed Petrol 60: 53–58

Milliken KL, Laubach SE (2000) The role of brittle deformation in sandstone diagenesis and fracture in siliciclastic petroleum reservoirs. In: *Pagel M, Barbin V, Blanc Ph, Ohnenstetter D* (eds) Cathodoluminescence in geosciences. Springer, Berlin Heidelberg New York Tokyo, pp 225–243

Moiseev BM (1985) Natural radiation processes in minerals (in Russ). Nedra, Moscow

Morad S, Bhattacharyya A, Al-Aasm IS, Ramseyer K (1991) Diagenesis of quartz in the Upper Proterozoic Kaimur sandstones, Son Valley, central India. Sed Geol 73: 209–225

Müller A, Seltmann R, Behr H-J (2000) Application of cathodoluminescence to magmatic quartz in a tin granite – case study from the Schellerhau granite complex, eastern Erzgebirge, Germany. Mineral Deposita 35: 169–189

Nassau K, Prescott BE (1975) A reinterpretation of smoky quartz. Phys Stat Sol 29: 659–663

Nettar D, Villafranca JJ (1985) A program for EPR powder spectra simulation. J Magn Res 64: 61

Neuser RD, Richter DK, Vollbrecht A (1989) Natural quartz with brown/violet cathodoluminescence – genetic aspects evident from spectral analysis. Zbl Geol Paläont Teil 1, H 7/8: 919–930

Neuser RD, Bruhn F, Götze J, Habermann D, Richter DK (1995) Kathodolumineszenz: Methodik und Anwendung. Zbl Geol Paläont Teil I, H 1/2: 287–306

Nutall RHD, Weil JA (1980) Two hydrogenic trapped-hole species in α-quartz. Solid State Comm 33: 99–102

Owen MR (1984) Sedimentary petrology and provenance of the upper Jackfork sandstone (Morrowan), Ouachita mountains, Arkansas. Thesis, University of Ilinois, Urbana, 154 p

Owen MR (1988) Radiation-damage halos in quartz. Geology 16: 529–532

Owen MR (1991) Application of cathodoluminescence to sandstone provenance. In: *Barker CE, Kopp OC* (eds) Luminescence microscopy: quantitative and qualitative aspects. SEPM, Dallas/Texas, pp 67–76

Owen MR, Anders MH (1988) Evidence from cathodoluminescence for non-volcanic origin of shocked quartz at the Cretaceous/Tertiary boundary. Nature 334/6178: 145–147

Pagel M, Barbin V, Blanc P, Ohnenstetter D (eds) (2000) Cathodoluminescence in geosciences. Springer, Berlin Heidelberg New York Tokyo, 514 p

Perny B, Eberhardt P, Ramseyer K, Mullis J, Pankrath R (1992) Microdistribution of Al, Li, and Na in α-quartz: possible causes and correlation with short-lived cathodoluminescence. Am Mineral 77: 534–544

Plötze M (1995) EPR-Untersuchungen an Quarz, Scheelit und Fluorit aus hochthermalen Seltenmetallvererzungen. Thesis, TU Bergakademie Freiberg, 141 p (unpublished)

Plötze M, Wolf D (1996) EPR- und TL-Spektren von Quarz: Bestrahlungsabhängigkeit der $[TiO_4^-/Li^+]^0$-Zentren. Eur J Mineral 8, Bh 1: 217

Pott GT, McNicol BD (1971) Spectroscopic study of the coordination and valence of Fe and Mn ions in and on the surface of aluminas and silicas. Disc Faraday Soc 52: 121–131

Rakov TL, Moiseev MB (1977) Paleodosimetric behaviour of E_1' centers in quartz (in Russ). Dokl AN USSR, ser geol 4: 679–682

Ramseyer K, Mullis J (1990) Factors influencing short-lived blue cathodoluminescence of alpha-quartz. Am Mineral 75: 791–800

Ramseyer K, Baumann J, Matter A, Mullis J (1988) Cathodoluminescence colours of alpha-quartz. Mineral Mag 52: 669–677

Ramseyer K, AlDahan AA, Collini B, Landström O (1992) Petrological modifications in granitic rocks from the Siljan impact structure: evidence from cathodoluminescence. Tectonophysics 216: 195–204

Remond G, Cesbron F, Chapoulie R, Ohnenstetter D, Roques-Carmes C, Schvoerer M (1992) Cathodoluminescence applied to the microcharacterization of mineral materials: a present status in experimentation and interpretation. Scann Micr 6: 23–68

Rink WJ, Rendell H, Marseglia EA, Luff BJ, Townsend PD (1993) Thermoluminescence spectra of igneous quartz and hydrothermal vein quartz. Phys Chem Minerals 20: 353–361

Ritter CJ, Dennen WH (1964) Colour center zonation in quartz. Geol Soc Am Bull 75: 915–916

Schneider N (1993) Das lumineszenzaktive Strukturinventar von Quarzphänokristen in Rhyolithen. Göttinger Arb Geol Paläont 60: 1–81

Serebrennikov AJ, Valter AA, Mashkovtsev RJ, Shcherbakova MYa (1982) The investigation of defects in shock-metamorphosed quartz. Phys Chem Mineral 8: 153–157

Seyedolali A, Krinsley DH, Boggs S, O'Hara PF, Dypvik H, Goles GG (1997) Provenance interpretation of quartz by scanning electron microscope-cathodoluminescence fabric analysis. Geology 25: 787–790

Siegel GH, Marrone MJ (1981) Photoluminescence in as-drawn and irradiated silica optical fibers: an assessment of the role of nonbridging oxygen defect centres. J Non-Cryst Solids 45: 235–247

Sippel RF, Spencer AB (1970) Luminescence petrography and properties of lunar crystalline rocks and breccias. Proc Apollo 11 Lunar Sci Conf, Vol 3: 2413–2426

Skuja LN, Entzian W (1986) Cathodoluminescence of intrinsic defects in glassy SiO_2, thermal SiO_2 films, and α-quartz. Phys Stat Sol (a) 96: 191–198

Sprunt ES, Dengler LA, Sloan D (1978) Effects of metamorphism on quartz cathodoluminescence. Geology 6: 305–308

Stevens Kalceff MA, Phillips MR (1995) Cathodoluminescence microcharacterization of the defect structure of quartz. Phys Rev B 52: 3122–3134

Stevens Kalceff MA, Phillips MR, Moon AR, Kalceff W (2000) Cathodoluminescence microcharacterization of silicon dioxide polymorphs. In: *Pagel M, Barbin V, Blanc P, Ohnenstetter D* (eds) Cathodoluminescence in geosciences. Springer, Berlin Heidelberg New York Tokyo, pp 193–224

Trukhin AN, Plaudis AE (1979) Investigation of intrinsic luminescence of SiO_2. Sov Phys Sol State 21: 644–646

Van den Kerkhoff AM, Müller A (1999) Retrograde trace element redistribution in quartz and fluid inclusion modification: observations by cathodoluminescence. Eur J Mineral 11, Bh 1: 121

Walker G (1985) Mineralogical applications of luminescence techniques. In: *Berry FJ, Vaughan DJ* (eds) Chemical bonding and spectroscopy in mineral chemistry. Chapman and Hall, London, pp 103–140

Walther H, Götze J (1993) Untersuchung von SiO_2-Zementen pedogener Silcretes mittels Kathodolumineszenz. Eur J Mineral 5, Bh 1: 55

Walther HB, Götze J, Wopfner H (1996) Silica cements in Central Australian silcretes. Intern Conf CL Rel Techn, Nancy, Abstracts, pp 165–166

Watt GR, Wright P, Galloway S, McLean C (1997) Cathodoluminescence and trace element zoning in quartz phenocrysts and xenocrysts. Geochim Cosmochim Acta 61: 4337–4348

Weil JA (1984) A review of electron spin spectroscopy and its application to the study of paramagnetic defects in crystalline quartz. Phys Chem Minerals 10: 149–165

Weil JA (1993) A review of the EPR spectroscopy of the point defects in α-quartz: the decade 1982–1992. In: *Helms CR, Deal BE* (eds) Physics and chemistry of SiO_2 and the Si–SiO_2 interface 2. Plenum Press, New York, pp 131–144

Yang XH, McKeever SWS (1990) Point defects and the pre-dose effect in quartz. Radiat Protect Dosim 33: 27–30

Zinkernagel U (1978) Cathodoluminescence of quartz and its application to sandstone petrology. Contrib Sed 8: 1–69

Authors' addresses: Dr. *J. Götze* (corresponding author), TU Bergakademie Freiberg, Department of Mineralogy, Brennhausgasse 14, D-09596 Freiberg, Federal Republic of Germany, e-mail: goetze@mineral.tu-freiberg.de; Dr. *M. Plötze*, ETH Zürich, Department of Geotechniques, CH-8093 Zürich, Switzerland; Dr. *D. Habermann*, TU Bergakademie Freiberg, Department of Experimental Physics, Silbermannstrasse 1, D-09596 Freiberg, Federal Republic of Germany